SCHACHTSCHNEIDER, J. H. & SNYDER, R. G. (1963). *Spectrochim. Acta*, **19**, 117–168.
SCHOMAKER, V. & TRUEBLOOD, K. N. (1968). *Acta Cryst.* B**24**, 63–76.
SEGERMAN, E. (1965). *Acta Cryst.* **19**, 789–796.
SHIPLEY, G. G. (1986). In *The Handbook of Lipid Research* 4 (*The Physical Chemistry of Lipids*), edited by DONALD M. SMALL, Ch. 5. New York: Plenum Press.
TASUMI, M., SHIMANOUCHI, T. & MIYAZAWA, T. (1963). *J. Mol. Spectrosc.* **11**, 422–432.
TEMPLETON, L. K. & TEMPLETON, D. H. (1973). *Abstr. Am. Cryst. Assoc. Meeting*, p. 143. Storrs, CT, USA.
WEBER, H.-P., CRAVEN, B. M. & MCMULLAN, R. K. (1983). *Acta Cryst.* B**39**, 360–366.
WEBER, H.-P., CRAVEN, B. M., SAWZIK, P. & MCMULLAN, R. K. (1991). *Acta Cryst.* B**47**, 116–127.

Acta Cryst. (1994). B**50**, 703–707

Dimethylaminobenzonitrile: Structure of the Lower-Temperature Solid Phase. Comparison with the Structure of the Higher-Temperature Phase and Correlation with Optical Spectroscopic Properties

BY GEOFFREY B. JAMESON, BASHIR M. SHEIKH-ALI AND RICHARD G. WEISS

Department of Chemistry, Georgetown University, Washington, DC 20057, *USA*

(*Received* 30 *August* 1993; *accepted* 8 *March* 1994)

Abstract

The crystal and molecular structures of 4-(*N*,*N*′-dimethylamino)benzonitrile (DMABN), $C_9H_{10}N_2$, in its lower-temperature solid phase at 173 K are reported and compared with those in the higher-temperature solid phase at 301 K. The molecular packing arrangement is correlated with some optical spectroscopic properties of the crystal.

Introduction

The intriguing photophysical properties of dialkylaminobenzonitriles [typified by the classic example *p*-(*N*,*N*′-dimethylamino)benzonitrile (DMABN)] have been investigated for more than 30 years (Lippert, Lüder & Boos, 1962). This interest has largely been driven by attempts to understand the structural and electronic features of dimethylaminobenzonitriles (and other molecules), which exhibit dual fluorescence bands, presumably *via* interconversion of twisted intramolecular charge-transfer (TICT) and untwisted locally excited (LE) states (see scheme below) (Rotkiewicz, Grellmann & Grabowski, 1973; Siemiarczuk, Grabowski, Krowczynski, Asher & Ottolenghi, 1977). Surprisingly, and in spite of the acknowledged dependence of ground-state conformations and configurations on the nature of the emitting excited states (Rettig, 1988), only last year has the crystalline structure of DMABN been published (Gourdon *et al.*, 1993; Heine, Herbst-Irman, Stalke, Kuhnle & Zachariasse, 1994), and only in the higher-temperature solid phase.

Here, we report the structure and unit-cell packing of DMABN in its lower-temperature solid phase and compare these with those of the higher-temperature phase. We have also duplicated the reported higher-temperature phase results. Although there are surprisingly minor differences in the conformation of molecules in the two phases, the unit-cell dimensions are very different. Both the crystal structures and their modes of packing provide insights concerning the photophysical data, especially in the solid state.

Experimental

Monoclinic crystals, m.p. 348–349 K (ref. m.p. 346–348 K; Rotkiewicz, Leismann & Rettig, 1989), were prepared by slow evaporation of a solution of doubly-sublimed DMABN (Aldrich, 98%) in hexane/ether. A reversible phase transition (confirmed to be solid–solid by optical microscopy) was detected at 261.1 K ($\Delta H = 6.3$ J g^{-1}) by differential scanning calorimetry.

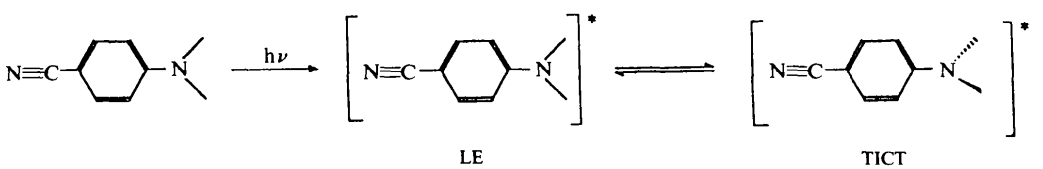

Table 1. *Crystal data and structure refinement for DMABN*

Empirical formula	$C_9H_{10}N_2$	
Formula weight	146.19	
Temperature (K)	173 (1)	301 (1)
Wavelength (Å)	0.71073	
Space group (crystal system)	$P2_1/c$ (monoclinic)	$P2_1/c$ (monoclinic)
Unit-cell dimensions		
a (Å)	7.022 (1)	6.312 (2)
b (Å)	7.597 (1)	7.933 (3)
c (Å)	15.812 (2)	17.216 (5)
β (°)	90.88 (1)	91.58 (2)
Volume (Å^3)	843.4 (3)	861.7 (5)
No. of reflections for cell	45	33
θ range for cell (°)	4.7–13.0	5–13
Z	4	4
D_{calc} (g cm^{-3})	1.151	1.127
Absorption coefficient (no correction, mm^{-1})	0.071	0.069
F	312	312
Crystal size (mm)	0.30 × 0.20 × 0.10	0.40 × 0.15 × 0.15
Diffractometer	Siemens $P4/RA$ with LT-2	
θ range for data collection (°)	2.90–25.63	2.83–25.00
Index ranges	$-1 \le h \le 8$, $-1 \le k \le 9$, $-18 \le l \le 19$	$-1 \le h \le 7$, $-1 \le k \le 9$, $-20 \le l \le 20$
No. of standard reflections (internal)	3 (every 97 reflections)	3 (every 97 reflections)
Variation in intensity	None detected	None detected
Scan type		ω
Scan range (°)	3.6	1.8
Reflections collected	2174	2200
Independent reflections	1477 (R_{int} = 0.0332)	1494 (R_{int} = 0.1865)
No. of observed reflections [$I > 2\sigma(I)$]	1135	428
Refinement method	Full-matrix least squares on F^2	
Data/restraints/parameters	1471/0/104	1481/0/102
Goodness-of-fit on F^2	1.015	0.994
Final R indices [$I > 2\sigma(I)$]	$R1$ = 0.0437, $wR2$ = 0.1099	$R1$ = 0.0790, $wR2$ = 0.1536
R indices (all data)	$R1$ = 0.0624, $wR2$ = 0.1314	$R1$ = 0.3177, $wR2$ = 0.3190
$(\Delta/\sigma)_{max}$	0.039	0.025
Weighting scheme	$w = 1/[\sigma^2(F_o^2) + (0.0620p)^2 + 0.19p]$ where $p = [\max(F_o^2, 0) + 2F_c^2]/3$	$w = 1/[\sigma^2(F_o^2) + (0.10p)^2]$
Largest diff. peak and hole (e Å^{-3})	0.130 & −0.164	0.078 & −0.090

Table 2. *Atomic coordinates* ($\times 10^4$) *and equivalent isotropic displacement parameters* (Å$^2 \times 10^3$) *for DMABN at* 173 K

$U_{eq} = (1/3)\sum_i\sum_j U_{ij} a_i^* a_j^* \mathbf{a}_i.\mathbf{a}_j$.

	x	y	z	U_{eq}
C(1)	4196 (2)	1782 (2)	1545 (1)	36 (1)
C(2)	4681 (2)	2639 (2)	2296 (1)	40 (1)
C(3)	3520 (2)	2569 (2)	2988 (1)	38 (1)
C(4)	1767 (2)	1659 (2)	2947 (1)	32 (1)
C(5)	1299 (2)	778 (2)	2185 (1)	34 (1)
C(6)	2492 (2)	834 (2)	1500 (1)	35 (1)
C(7)	5448 (3)	1863 (2)	835 (1)	45 (1)
C(8)	1175 (3)	2400 (3)	4425 (1)	49 (1)
C(9)	−1190 (3)	660 (3)	3589 (1)	46 (1)
N(1)	570 (2)	1656 (2)	3621 (1)	37 (1)
N(2)	6462 (3)	1933 (3)	275 (1)	64 (1)

Table 3. *Anisotropic displacement parameters* (Å$^2 \times 10^3$) *for DMABN at* 173 K

The anisotropic displacement factor exponent takes the form: $-2\pi^2[(ha^*)^2 U_{11} + ... + 2hka^*b^*U_{12}]$.

	U_{11}	U_{22}	U_{33}	U_{23}	U_{13}	U_{12}
C(1)	40 (1)	32 (1)	36 (1)	5 (1)	7 (1)	6 (1)
C(2)	35 (1)	37 (1)	47 (1)	1 (1)	3 (1)	−4 (1)
C(3)	41 (1)	38 (1)	36 (1)	−4 (1)	1 (1)	−5 (1)
C(4)	35 (1)	28 (1)	32 (1)	2 (1)	2 (1)	3 (1)
C(5)	35 (1)	30 (1)	36 (1)	0 (1)	0 (1)	−2 (1)
C(6)	43 (1)	32 (1)	31 (1)	−1 (1)	1 (1)	3 (1)
C(7)	48 (1)	41 (1)	46 (1)	3 (1)	10 (1)	3 (1)
C(8)	50 (1)	62 (1)	34 (1)	−7 (1)	5 (1)	−7 (1)
C(9)	43 (1)	50 (1)	45 (1)	−4 (1)	11 (1)	−8 (1)
N(1)	40 (1)	39 (1)	33 (1)	−3 (1)	6 (1)	−5 (1)
N(2)	65 (1)	70 (1)	59 (1)	3 (1)	27 (1)	0 (1)

Crystal data and salient features of structure solution and refinement for the lower and upper temperature phases of DMABN are provided in Table 1. Table 2 gives final atomic positional parameters and Table 3 atomic displacement parameters for the low-temperature phase.* Parameters for the room-temperature phase are very similar to those previously reported (Gourdon *et al.*, 1993; Schuddeboon *et al.*, 1992; Heine, Herbst-Irman, Stalke, Kuhnle & Zachariasse, 1994) and are available as supplementary material. Since DMABN does not crystallize well, several crystals were tested before suitable ones were identified. For the data collection at 173 K, the crystal was secured to a glass fiber by epoxy resin (*sans* hardener); for the data collection at 301 K, the crystal was sequestered in a thin-walled glass capillary, along with additional DMABN, since it was found that at this temperature unprotected crystals of DMABN sublime rather rapidly in the X-ray beam. At 302 K, all H atoms of DMABN could be located in a difference Fourier map, although it was apparent that methyl H atoms were almost freely rotating. At 173 K, notwithstanding very poor crystal mosaicity as a result of the phase transition that necessitated a 3.6° scan width in ω data collection, diffraction intensity persisted more significantly to a higher angle; methyl H atoms were well ordered. The structure at 173 K was determined by Patterson rotation–translation search methods (*PATSEE*) after more usual (*SHELXS*, *SHELXTL*) methods failed in our hands (Sheldrick, 1994). The structure was subsequently determined at 301 K. H atoms were constrained to ride on their attached C atoms with appropriate standard stereochemistries and with iso-

* Lists of structure factors, anisotropic displacement parameters & H-atom coordinates have been deposited with the IUCr (Reference: GR0328.) Copies may be obtained through The Managing Editor, International Union of Crystallography, 5 Abbey Square, Chester CH1 2HU, England.

tropic temperature factors equal to 1.5 times U_{eq} for methyl H atoms and 1.2 times U_{eq} for phenyl H atoms.

Emission and excitation spectra were recorded in a front-face arrangement using a SPEX 111 fluorimeter equipped with a 150 W Xenon lamp. The absorption spectra of the same samples were recorded on a Perkin–Elmer lambda 6 spectrometer.

Results and discussion

Bond distances and angles for the molecule at 173 and 301 K are given in Table 4 and a diagram of the crystal structure at 173 K is provided in Fig. 1. The unit cell and structural parameters we found at 301 K agree well with those reported previously (Gourdon *et al.*, 1993; Schuddeboon *et al.*, 1992; Heine, Herbst-Irman, Stalke, Kuhnle & Zachariasse, 1994). The DMABN molecule in both phases adopts a nearly planar conformation: the pyramidalization at the amino N atom is 0.072 Å at 173 K and 0.079 Å at 301 K. With reference to the more precise low-temperature structure, evidence exists for some pseudo-quinoid character to the phenyl ring: the N_{amino}—C_{phenyl} bond at 1.366 (2) Å is much shorter than a standard C_{sp^2}—N bond; the C—C bonds involving the amino-substituted C atom average 1.413 (2) Å, which is longer than the standard aromatic C—C bond length of 1.392 Å; the pair of bonds adjacent to those mentioned above average only 1.377 (3) Å. In addition, the internal angle at the amino-substituted C atom is 117.6 (1)°. Thus, the lone pair of electrons on the amino N atom reside in an almost pure *p*-orbital, which is well conjugated with the aromatic ring.

On the other hand, there is little structural evidence for conjugation of the cyano group with the phenyl ring: the pair of bonds involving the cyano-substituted C atom average 1.394 (7) Å – the inequality in the two distances is at the margin of significance – and the internal angle is 118.3 (1)°. This molecule offers, then, a contrast between perturbations of phenyl ring π-electron delocalization

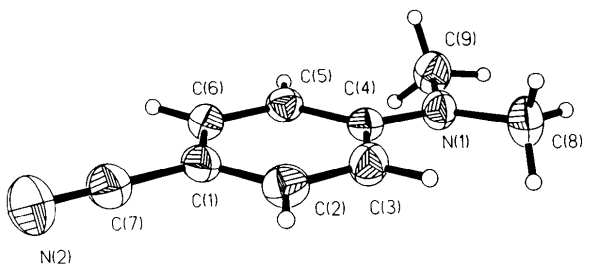

Fig. 1. *ORTEP*-type (Johnson, 1965) diagram of DMABN at 173 K. Ellipsoids are drawn at the 50% probability level.

Table 4. *Bond lengths* (Å) *and angles* (°) *for DMABN*

	301 K	173 K
C(4)—N(1)	1.356 (5)	1.366 (2)
C(4)—C(5)	1.390 (6)	1.411 (2)
C(4)—C(3)	1.400 (6)	1.414 (2)
N(1)—C(8)	1.459 (6)	1.447 (2)
N(1)—C(9)	1.436 (5)	1.450 (2)
C(5)—C(6)	1.377 (6)	1.379 (2)
C(6)—C(1)	1.381 (6)	1.399 (2)
C(7)—N(2)	1.152 (6)	1.145 (2)
C(7)—C(1)	1.425 (7)	1.436 (2)
C(1)—C(2)	1.394 (6)	1.389 (2)
C(3)—C(2)	1.356 (6)	1.375 (2)
N(1)—C(4)—C(5)	121.9 (6)	121.6 (2)
N(1)—C(4)—C(3)	121.6 (6)	120.8 (2)
C(5)—C(4)—C(3)	116.5 (5)	117.55 (14)
C(4)—N(1)—C(8)	121.1 (5)	120.38 (14)
C(4)—N(1)—C(9)	122.0 (5)	120.55 (14)
C(8)—N(1)—C(9)	116.0 (5)	118.29 (13)
C(6)—C(5)—C(4)	121.9 (5)	121.1 (2)
C(5)—C(6)—C(1)	120.8 (5)	120.4 (2)
N(2)—C(7)—C(1)	177.0 (7)	179.3 (2)
C(2)—C(1)—C(6)	117.7 (5)	118.92 (14)
C(2)—C(1)—C(7)	120.2 (6)	120.0 (2)
C(6)—C(1)—C(7)	122.1 (6)	121.1 (2)
C(2)—C(3)—C(4)	121.7 (6)	120.7 (2)
C(3)—C(2)—C(1)	121.4 (6)	121.2 (2)

wrought by a dimethylamino group, whose Hammett σ-constant is dominated by resonance contributions, and the minimal perturbations caused by a cyano group, whose Hammett σ-constant is heavily weighted in favour of the inductive terms: for —NMe_2, $\sigma_I = 0.06$ and $\sigma_R = -0.52$; for —CN, $\sigma_I = 0.57$ and $\sigma_R = 0.13$ (Exner, 1988). Treatment of these structural Hammett parameters according to the methods of Krygowski (1984, 1987) leads to the prediction that DMABN in its electronic ground state has as much quinoid character as *p*-aminobenzonitrile ($\sum\Delta = -5.3$ and -5.4 pm, respectively).

There are several small, but significant, differences in the molecular conformation of DMABN at 173 and 301 K. Whereas the extent of pyramidalization is insignificantly different between the two phases, the rotation of the dimethylamino group about the C_{phenyl}—N_{amino} bond differs significantly: at room temperature, there is little rotation (C_{phenyl}—C_{phenyl}—N_{amino}—C_{methyl} angles of -5.1 and 5.6°), while at the lower temperature the dimethylamino group is rotated about 4.4° (torsion angles of -7.7 and 3.3°). The dihedral angle between the dimethylamino and phenyl planes is 9.9° at 301 K (mostly a consequence of pyramidalization at the amino nitrogen) and 7.1° at 173 K.

The transition from the room-temperature phase to the lower-temperature phase is accompanied by a significant reorganization of molecular packing, which can be characterized crudely as a slippage of alternating molecules and consequent compression along the orthogonal directions. Although the

overall decrease in unit-cell volume of 2.1% (18.3 Å^3) is unremarkable, it is comprised of an 11.2% (0.71 Å) *increase* in the *a* axis, an 8.2% (1.40 Å) *decrease* in the *c* axis and a 4.2% *decrease* (0.34 Å) in the *b* axis. Changes this large on phase transition usually lead to a polycrystalline product. At the molecular level, the molecules in both phases are arranged in a staggered antiparallel herring-bone manner. There is no consequential π–π type overlap of parallel aromatic planes, in spite of the molecular long axes being parallel; the phenyl rings are inclined 66.68° to one another at 301 K and 69.2° at 173 K.

Relative to the symmetry axes and centers, which are preserved in the two phases, and comparing the crystal structure at 173 K to that at 301 K, molecules of the 2_1-screw-related pair move closer together in the *a* direction and further apart in the *c* direction. This is illustrated in Fig. 2, where the room temperature structure in projection down the *b* axis has a more pronounced zigzag arrangement than does the lower-temperature structure. The centroids of screw-related phenyl rings are separated by 4.793 Å at 173 K and 4.762 Å at 301 K; for pairs of DMABN molecules related by inversion centers, there is a 0.520 Å decrease in the separation of centroids across the inversion centers that places cyano groups adjacent, offset by a 1.436 Å increase in the separation of centroids across inversion centers that places methyl groups adjacent.

Notwithstanding the rearrangement of the centroids of molecules, intermolecular contact distances among atoms remain surprisingly similar. $C_{cyano}\cdots N'_{cyano}$ and $C_{cyano}\cdots C'_{cyano}$ intermolecular separations are essentially equivalent in the phases [3.647 (6) Å at 301 K and 3.622 (2) Å at 173 K; 3.898 (6) and 3.913 (2) Å, respectively], but the $N_{cyano}\cdots N'_{cyano}$ separation increases slightly from 3.681 (2) Å at 173 K to 3.749 (6) Å at 301 K. While the centrosymmetrically related amino N atoms move 0.611 Å closer (5.711 Å at 301 K and 5.100 Å at 173 K), because of intramolecular and intermolecular rotations of the dimethylamino moieties, the closest contacts of the amino methyl groups with the surrounding atoms remain remarkably similar – at 301 K, $C_{methyl}\cdots N'_{cyano} = 3.675$ and 3.594, $C_{methyl}\cdots C'_{phenyl} = 3.670$ and $C_{methyl}\cdots C'_{methyl} = 4.298$ Å; at 173 K, $C_{methyl}\cdots N'_{cyano} = 3.645$ and 3.629, $C_{methyl}\cdots C'_{phenyl} = 3.630$ and $C_{methyl}\cdots C'_{methyl} = 3.902$ Å. The origin of the phase transition is not clear. The U_{eq} values for the methyls are rather similar in magnitude to those of the N atom to which they are attached. On this basis, it is unlikely that freezing of the motions associated with the inversion of the dimethylamino groups is responsible for the phase transition. Although we favor attenuation of

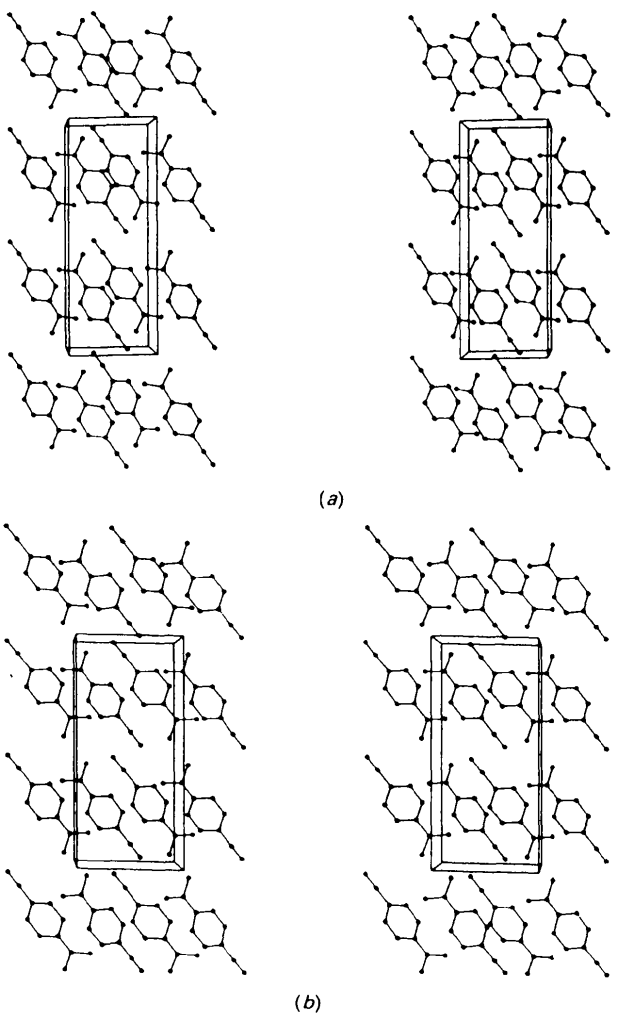

Fig. 2. Packing diagram of DMABN at (*a*) 301 and (*b*) 173 K, viewed down the *b* axis.

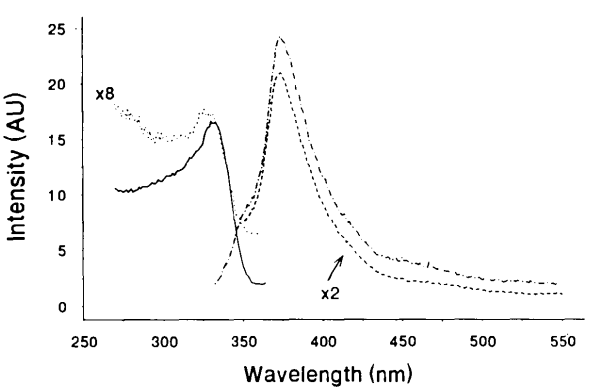

Fig. 3. Excitation spectra of DMABN monitored at 380 (—) and 450 nm (...) and emission specta excited at 280 (– · – · –) and 340 nm (– – –) at room temperature.

rotation about the C_{methyl}—N bonds as the major factor, there is no firm evidence to support this either.

The closest $N_{cyano}\cdots N'_{amino}$ distances are 4.037 (at 301 K) and 4.066 Å (at 173 K). The closest $H\cdots X'$ contacts (2.75–2.76 Å at 173 K and 2.81–2.83 Å at 301 K, where $X = C$, N) all involve the cyano N atom with three H atoms from two (different) methyl and one phenyl moieties.

A study of the emission from crystalline DMABN at 293 K has been performed (Rotkiewicz, Leismann & Rettig, 1989). Luminescence has been attributed to monomer fluorescence, phosphorescence and fluorescence from excited-state aggregates. Ground-state dimers of DMABN were not considered likely based upon these and related spectroscopic observations (Rotkiewicz, Leismann & Rettig, 1989). The general position of the fluorescence maximum is much more consistent with emission from an LE than a TICT state (Rotkiewicz, Grellmann & Grabowski, 1973; Rettig, 1988). Thus, the 'untwisted' structure of DMABN in the higher-temperature phase either cannot (due to a dearth of free volume) or prefers not to (due to the local electrostatic fields experienced) twist within the crystalline lattice. Our room-temperature emission spectra from finely powdered crystals of DMABN sandwiched between quartz plates (Fig. 3) are in fair agreement with the previously published paper, given the fact that our sample was not deoxygenated; however, there are significant differences, which include the absence of bands attributed to phosphorescence and an emission maximum at 370 nm, which is *ca* 10 nm less than the previously reported value (Rotkiewicz, Leismann & Rettig, 1989). Our corresponding UV–vis absorption and excitation spectra exhibit a broad, plateau-like maximum at *ca* 300–325 nm (Fig. 3); only the excitation spectra are shown for clarity. Both the excitation and absorption maxima are red-shifted compared with dilute solution spectra, but they are also more compatible with forced aggregates than discrete ground-state complexes.

Concluding remarks

As mentioned above, the unit cell of the lower-temperature solid phase has very different dimensions from those of the higher-temperature phase. Additionally, there are subtle, but important, structural differences for individual DMABN molecules. Most notably, the molecular packing in both phases does not appear to depend strongly upon π–π interactions between neighboring molecules. While dipole–dipole interactions* may be responsible for the antiparallel orientation between vicinal DMABN molecules (Schuddeboon *et al.*, 1992; Vasil'eva, Bozov & Geiderikh, 1959), the lack of close contacts and attractive orbital interactions of the π-systems indicates that the molecules are relatively isolated in an electronic sense. The solid-state absorption and emission spectra are consistent with this interpretation, since there is no hint of excition-splitting bands (Kasha, 1976) which can occur when pairs (or more) of molecules interact strongly with nonparallel transition dipoles.

We thank the National Science Foundation for financial support (CHE-9213622) and for funding for the diffractometer (CHE-9115394), Dr Klaas Zachariasse of the Max-Planck-Institut für Biophysikalische Chemie, Göttingen, for sharing unpublished data and Mr Peter Kamaras for technical assistance.

* The dipole moment of DMABN at 298 K in 1,4-dioxane and benzene is 6.6 D (Vasil'eva, Bozov & Geiderikh, 1959; Schuddeboon *et al.*, 1992).

References

EXNER, O. (1988). *Correlation Analysis of Chemical Data*, pp. 143 ff. Prague: Plenum Press.

GOURDON, A., LAUNAY, J.-P., BUJOLI-DOEUFF, M., HEISEL, F., MIEHÉ, J. A., AMOUYAL, E. & BOILLOT, M.-L. (1993). *J. Photochem. Photobiol. A*, **71**, 13–25.

HEINE, A., HERBST-IRMAN, R., STALKE, D., KUHNLE, W. & ZACHARIASSE, K. A. (1994). *Acta Cryst.* **B50**, 363–373.

JOHNSON, C. K. (1965). *ORTEP*. Report ORNL-3794. Oak Ridge National Laboratory, Tennessee, USA.

KASHA, M. (1976). *Spectroscopy of the Excited State*, edited by B. DIBARTOLE, pp. 337–363. New York: Plenum Press.

KRYGOWSKI, T. M. (1984). *J. Chem. Res.* pp. 238–239.

KRYGOWSKI, T. M. (1987). *J. Chem. Res.* pp. 120–121.

LIPPERT, E., LÜDER, W. & BOOS, H. (1962). *Advances in Molecular Spectroscopy*, edited by A. MANGINI, pp. 443–457. Oxford: Pergamon Press.

RETTIG, W. (1988). *Appl. Phys. B*, **45**, 145–149.

ROTKIEWICZ, K., GRELLMAN, K. H. & GRABOWSKI, Z. R. (1973). *Chem. Phys. Lett.* **19**, 315–318; **21**, 212.

ROTKIEWICZ, K., LEISMANN, H. & RETTIG, W. (1989). *J. Photochem. Photobiol. A*, **49**, 347–367.

SCHUDDEBOON, W., JONKER, S. A., WARMAN, J. M., LEINHOS, U., KÜHNLE, W. & ZACHARIASSE, K. A. (1992). *J. Phys. Chem.* **96**, 10809–10819.

SHELDRICK, G. M. (1994). *J. Appl. Cryst.*, in preparation.

SIEMIARCZUK, A., GRABOWSKI, Z. R., KROWCZYNSKI, A., ASHER, M. & OTTOLENGHI, M. (1977). *Chem. Phys. Lett.* **51**, 315–320.

VASIL'EVA, V. N., BOZOV, V. P. & GEIDERIKH, M. A. (1959). *Russ. J. Phys. Chem.* **33**, 32–34.